JAIST Repository
https://dspace.jaist.ac.jp/

Title	Antenna Doping: A Countermeasure Against MIMO Spatial Correlation
Author(s)	Kai, Yen; Karjalainen, J.; Matsumoto, T.
Citation	IEEE 65th Vehicular Technology Conference, 2007. VTC2007-Spring.: 2450-2454
Issue Date	2007-04
Type	Conference Paper
Text version	publisher
URL	http://hdl.handle.net/10119/4836
Rights	Copyright (c)2007 IEEE. Reprinted from IEEE 65th Vehicular Technology Conference, 2007. VTC2007-Spring. This material is posted here with permission of the IEEE. Such permission of the IEEE does not in any way imply IEEE endorsement of any of JAIST's products or services. Internal or personal use of this material is permitted. However, permission to reprint/republish this material for advertising or promotional purposes or for creating new collective works for resale or redistribution must be obtained from the IEEE by writing to pubs-permissions@ieee.org. By choosing to view this document, you agree to all provisions of the copyright laws protecting it.
Description	

JAIST
JAPAN
ADVANCED INSTITUTE OF
SCIENCE AND TECHNOLOGY

Japan Advanced Institute of Science and Technology

Antenna Doping: A Countermeasure Against MIMO Spatial Correlation

Kai Yen
Institute for Infocomm Research
21 Heng Mui Keng Terrace, Singapore 119613
Email: yenkai@i2r.a-star.edu.sg

Juha Karjalainen and Tadashi Matsumoto
University of Oulu
P.O. Box 4500, FIN-90014 University of Oulu, Finland
Email: {juha.karjalainen,tadashi.matsumoto}@ee.oulu.fi

***Abstract*— In this paper, we address the problem of multiple-input multiple-output (MIMO) spatial multiplexing (SM) systems in the presence of antenna fading correlation. It is well known that severe spatial correlations present at the transmitter and/or receiver can significantly compromise the performance of existing SM systems. Recent results showed that joint-over-antenna (JA) iterative detection schemes can improve the performance of SM systems in correlated channels as compared to schemes that detected the signals on an antenna-by-antenna basis. We extend this idea in this paper by incorporating a so-called antenna doping (AD) scheme into the SM system, in order to further counteract the detrimental effects of spatial correlation. Through simulations, we show that AD can improve the performance by 3-4 dB in severe spatial correlation as compared to non-doping systems. This improvement is explained with the aid of extrinsic information transfer (EXIT) charts, which illustrate the convergence behavior of the JA iterative detection with and without AD.**

I. Introduction

Multiple-input multiple-output (MIMO) spatial multiplexing (SM) systems, employing several transmit and receive antennas, are capable of achieving a significant increase in capacity as compared to traditional single antenna systems [1], [2]. This achievement is dependent upon the assumption that the different transmit-receive antenna pairs are subjected to uncorrelated fading. In practice, however, signal correlation exists among the antenna elements in realistic environments. Because correlated MIMO channels possess fewer degrees of freedom as compared to independent and identically distributed (i.i.d.) channels, studies have shown that severe spatial correlations present at the transmitter and/or receiver can significantly compromise the performance of SM systems [3].

In order to suppress the detrimental effects of spatial correlation, Gore *et al.* proposed a transmit selection algorithm that either maximizes the average throughput or minimizes the average probability of error for SM systems having transmit spatial correlation [4]. Further performance improvement of SM systems in correlated fading can be achieved by varying the number of transmit antennas as well as the symbol constellations, as proposed by Narasimhan [5]. A fast Fourier transform based antenna selection scheme was shown by Molisch *et al.* to perform better than conventional antenna selection schemes in spatially correlated MIMO channels [6]. Instead of antenna selection, the performance of SM systems in spatially correlated channels can be improved by precoding the signal before transmission. Through numerical optimization, power allocation and relative phase adjustment between the multiplexed symbol streams was shown by Nabar *et al.* to increase the multipelxing gain [7]. Akhtar *et al.* introduced a closed-form precoder, which also adjusts the power and phase shifts of each stream, without requiring the need for any complex numerical optimization [8]. These proposed techniques mentioned above rely on the fact that knowledge of the channel correlation statistics must be made available at the transmitter/receiver. Recently, Karjalainen *et al.* proposed an iterative frequency domain joint-over-antenna (JA) signal detection technique, which was shown to achieve a lower bit error rate (BER) as compared to similar iterative techniques that detect the spatially multiplexed signals on an antenna-by-antenna basis, without requiring any knowledge of the channel correlation statistics [9]–[11].

In this paper, we extend the JA-based detection scheme by incorporating a so-called antenna doping (AD) technique, to further improve the performance of SM systems in spatially correlated channels. The idea behind AD is similar to that of code doping, a technique proposed by ten Brink [12] for accelerating convergence and/or initiating the iterative decoding, by opening a 'tunnel' in the extrinsic information transfer (EXIT) chart [13]. With the aid of EXIT charts, we will show that in the presence of spatial correlation, AD builds up a tunnel at a lower signal-to-noise ratio (SNR) as compared to conventional SM systems. The presence of this tunnel suggests that decoding convergence can be initiated and hence this leads to an improvement in the BER performance. In severely correlated channels, AD can improve the BER performance by as much as 3-4 dB over SM systems. These gains will be demonstrated by simulations.

This paper is organized as follows. Following this introduction, we will first establish the channel model that will be considered throughout this paper in Section II. Next, a brief review of the conventional SM system will be given in Section III. The main feature of this paper is presented in Section IV, where we first highlight the motivation behind our AD proposal. We will then proceed to introduce two possible types of AD, namely inner AD and outer perfect AD. BER results and EXIT charts are also provided in this section to demonstrate the performance of AD in correlated fading channels. Finally, conclusions are given in Section V.

II. Channel Model

We consider a vertically encoded SM MIMO system with N_T transmit and N_R receive antennas for cyclic-prefix single carrier burst transmission [14]. The channel corresponding to each transmit-receive antenna pair is frequency-selective, quasi-static block Rayleigh fading consisting of L number of taps. The channel tap matrices are assumed to be i.i.d. of each other and only transmit correlation is present at each tap matrix while the receive antennas are uncorrelated. Hence, the lth tap MIMO channel matrix can be written as

$$\mathbf{H}_l = \overline{\mathbf{H}}_l \mathbf{R}_t^{\frac{1}{2}}, \quad l = 0, \ldots, L-1, \tag{1}$$

where $\overline{\mathbf{H}}_l$ is the $N_R \times N_T$ i.i.d. zero mean complex Gaussian matrix and $\mathbf{R}_t$ is the $N_T \times N_T$ transmit correlation matrix, which is given

1550-2252/$25.00 ©2007 IEEE

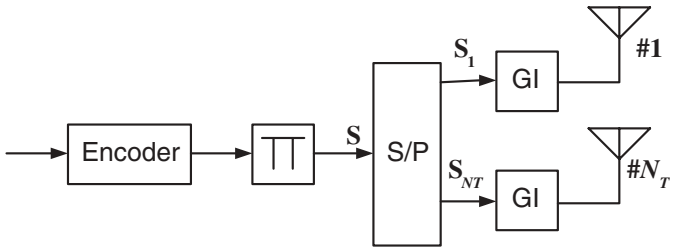

(a) Conventional spatial multiplexing transmitter.

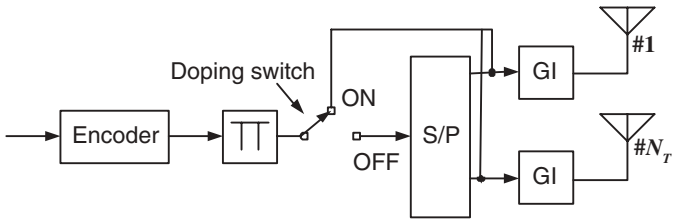

(b) Spatial multiplexing transmitter with inner antenna doping.

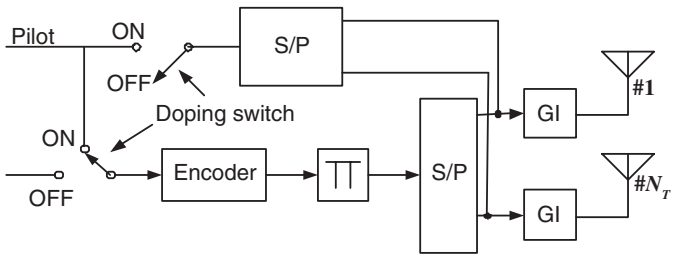

(c) Spatial multiplexing transmitter with outer perfect antenna doping.

Fig. 1: Spatial multiplexing transmitter structure with and without antenna doping.

by

$$\mathbf{R}_t = \begin{bmatrix} 1 & \rho_{1,2} & \cdots & \rho_{1,N_T} \\ \rho_{2,1} & 1 & \cdots & \rho_{2,N_T} \\ \vdots & \vdots & \ddots & \vdots \\ \rho_{N_T,1} & \rho_{N_T,2} & \cdots & 1 \end{bmatrix}, \tag{2}$$

with $\rho_{n,m}$ denoting the correlation coefficient between the nth and mth transmit antenna. For simplicity sake, we assumed that $\mathbf{R}_t$ is the same for all the channel tap matrices and that all transmit antennas pairs have the same correlation coefficient, i.e. $\rho_{i,j} = \rho \ \forall j \neq i$.

III. Conventional Spatial Multiplexing

The structure of the conventional SM transmitter is illustrated in Fig. 1(a). Let us denote a convolutional-encoded interleaved symbol stream of length N_TQ as $\mathbf{s} = [s(1), \ldots, s(N_TQ)]^{\mathrm{T}}$, where $(\cdot)^{\mathrm{T}}$ denotes transpose and $s(j), j = 1, \ldots, N_TQ$ is assumed to be a quadrature phase shift keying (QPSK)-modulated symbol during the jth symbol period in this paper. According to the figure, the symbol stream $\mathbf{s}$ is decomposed into N_T sub-streams, where the nth sub-stream is represented by a $1 \times Q$ vector $\mathbf{s}_n, n = 1, \ldots, N_T$. The elements in $\mathbf{s}_n$ comprise of the symbols $s(qN_T+n), q = 0, \ldots, Q-1$ in ascending order. A guard period of length G is then inserted by the guard insertion (GI) block in Fig. 1(a). As a result, the length of each layer is now given by $K = Q+G$, which is equivalent to the length of the discrete Fourier transform (DFT) employed by the frequency-domain equalizer [9]–[11] at the receiver. Since guard insertion is common in both the conventional SM transmitter as well as the SM system with antenna doping (see Fig. 1(b) and Fig. 1(c)), we shall ignore the guard period in our subsequent discourse. However, the guard period is still inserted in our simulations.

Number of Channel Taps	32
Modulation	QPSK
Channel Encoder	Convolutional Code $n = 2, k = 1, K = 3$ $G_0 = 7, G_1 = 5$
Channel Decoder	MAP Decoder
Interleaver	Random
Iterations	4
Number of Transmit Antennas N_T	4
Number of Receive Antennas N_R	4
Guard Per Antenna G	32 QPSK Symbols
DFT Length of Conventional SM Q	495

TABLE I: Standard simulation parameters used.

Let us introduce a $N_TQ \times N_TQ$ transformation matrix $\mathbf{W}_{\text{SM}}$ and a $1 \times N_TQ$ vector $\mathbf{x}_j = [\mathbf{0}_{1\times M}, 1, \mathbf{0}_{1\times N_TQ-M-1}]^{\mathrm{T}}, j = 1, \ldots, N_TQ$, where $\mathbf{0}_{1\times M}$ is a $1 \times M$ zero vector and $M = \text{mod}(j-1, N_T)Q + \left\lfloor \frac{j-1}{N_T} \right\rfloor$. Then we can express the transmitted layers over the N_T antennas as

$$\mathbf{b} = \mathbf{W}_{\text{SM}}\mathbf{s}, \tag{3}$$

where

$$\mathbf{W}_{\text{SM}} = [\mathbf{x}_1, \mathbf{x}_2, \ldots, \mathbf{x}_{N_TQ}] \tag{4}$$

and the $N_TK \times 1$ vector $\mathbf{b} = [\mathbf{s}_1, \ldots, \mathbf{s}_{N_T}]^{\mathrm{T}}$ has a form identical to that in [10, Eq. (2)], after the inclusion of the guard period. The application of the frequency domain JA turbo equalization for detecting $\mathbf{b}$ is well documented in [9]–[11] and hence the operation will not be treated here.

In order to clearly understand the motivation behind our AD proposal, let us first study the EXIT chart of the JA turbo equalization, as shown in Fig. 2, and envisage its convergence behavior when $\rho = 0.0, 0.99$ and 0.7. The standard parameters that we have used throughout our simulations are given in Table I. On the x-axis, I_{A1} and I_{E2} denote the mutual information of the *a priori* inputs to the JA equalizer and the extrinsic information at the output of the convolutional MAP decoder, respectively, while I_{E1} and I_{A2} on the y-axis denote the mutual information of the extrinsic information at the output of the JA equalizer and the *a priori* information to the convolutional MAP decoder. According to the figure, if there is no spatial correlation, a wide tunnel exists between the transfer characteristics of the JA equalizer and the convolutional MAP decoder at $E_b/N_0 = 5$ dB. This ensures that decoding convergence is initiated and hence a low BER is expected. However, when $\rho = 0.99$, a so-called pinch-off limit [13] is observed at about 18 dB as the transfer characteristics of the JA equalizer and the MAP decoder just intersects with each other at $I_{A1} \approx 0.3$. Hence, this suggests that decoding convergence can only be triggered for E_b/N_0 values above the pinch-off limit. Notice that when $\rho = 0.7$, a narrow tunnel exists at 5 dB. Hence decoding convergence can be initiated but more iterations is required, in order to achieve optimal performance. These claims can be validated by observing the BER performance of the SM system, as illustrated in Fig. 3. We can clearly see that when $\rho = 0.99$, convergence occurs only after 18 dB, which is the pinch-off limit as mentioned previously. Also, at 5 dB when $\rho = 0.7$, we can see that the BER is improving, albeit slowly, as the number of iterations is increased. This is due to the existence of a narrow tunnel, as shown in Fig. 2.

Having seen the decoding convergence behavior of the SM system at various spatial conditions, we will next highlight the motivation

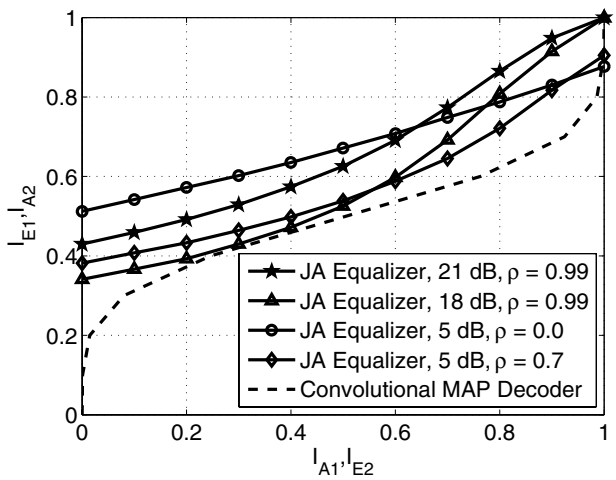

Fig. 2: EXIT chart of the JA turbo equalization in conventional SM system with various spatial correlations.

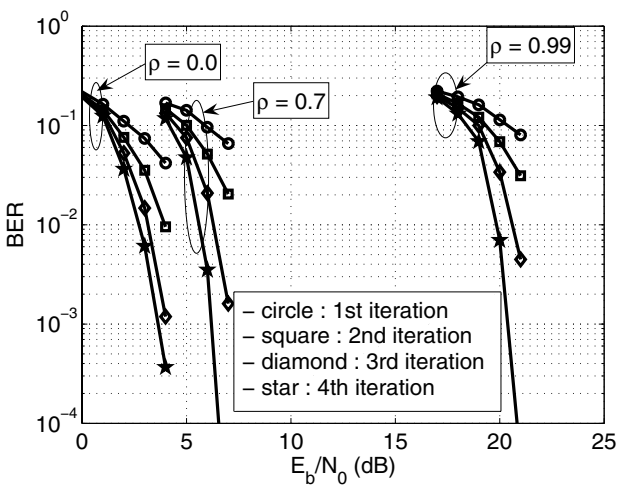

Fig. 3: BER performance of the SM system under various spatial correlations.

behind the AD scheme and show how AD can improve the performance by altering the EXIT chart. Two types of AD are introduced here, namely inner AD and outer perfect AD. However, due to space limitations, only inner AD will be thoroughly covered in this paper.

IV. Antenna Doping

The idea behind code doping was originated from ten Brink [12] when he observed that the transfer characteristics of rate 1 recursive convolutional codes start at the origin $I_{E1}(I_{A1} = 0) \approx 0$, which deters any iteration from taking place due to the lack of a tunnel. In order to trigger convergence, ten Brink proposed a code doping scheme to achieve $I_{E1}(0) > 0$ or $I_{E2}(0) > 0$, thereby creating a tunnel and hence permitting further iterations. In other words, code doping alters the transfer characteristics of the inner encoder or outer encoder (depending on the type of doping) so that decoding convergence can occur.

Motivated by this idea, we proposed the AD scheme. The purpose of AD is to alter the transfer characteristics of the JA equalizer or the convolutional MAP decoder such that a tunnel can be created at a lower SNR in the presence of spatial correlation. This will trigger decoding convergence and hence lowers the BER. Similar to ten Brink's code doping scheme, two types of doping are introduced here, namely inner AD and outer perfect AD.

A. Inner Antenna Doping

The transmitter structure of the SM system with inner AD (IAD) is shown in Fig. 1(b). As we can see, IAD can be easily incorporated into the SM transmitter by inserting a so-called doping switch before the serial-to-parallel (S/P) multiplexer. When the doping switch is in the 'OFF' position, the incoming coded symbols are decomposed into N_T independent sub-streams, which are then transmitted simultaneously. This scenario is equivalent to that of the conventional SM system highlighted previously. In the context of the AD system, these symbols are referred to as non-doping symbols.

On the other hand, if the doping switch is in the 'ON' position, the same coded symbol will be transmitted from all N_T antennas simultaneously. Such a symbol will be referred to as a doping symbol. The problem now is to determine the switching time of the doping switch between the 'ON' and 'OFF' state.

We define a so-called doping ratio, which is given as $1 : D$, where $D - 1$ should be a multiple of N_T. The doping ratio indicates that 1 out of every D symbols in $\mathbf{s}$ is a doping symbol[1] while there are $D-1$ non-doping symbols. In this paper, we assumed that the doping symbol is always the last symbol in a block of D symbols, without loss of generality. In other words, the symbols $s(nD)$, where n is an integer, are doping symbols. Obviously, the transmission of doping symbols from all the antennas leads to a loss in the spectral efficiency as compared to the conventional SM system. Let us denote the ratio of the average information bit power to noise power per receive antenna in the conventional SM system as E_b/N_0. Then the corresponding ratio in the IAD system will be given by

$$(E_b/N_0)_{\text{IAD}} = \frac{D}{N_T + D - 1}\,(E_b/N_0)\,. \tag{5}$$

Hence the loss in the spectral efficiency is minimal as the value of D is increased. However, as we shall see in our simulation results, the value of D has a direct impact on the performance of the IAD system, depending on the degree of spatial correlation.

In mathematical terms, we can easily express the inclusion of IAD by modifying the transformation matrix. Due to the doping symbols, the transformation matrix with antenna doping is now a $L \times N_T Q$ matrix $\mathbf{W}_{\text{IAD}}$, where $L = N_T Q\left(\frac{N_T-1}{D} + 1\right)$. After the guard insertion, the length of each sub-stream is now $K' = Q\left(\frac{N_T-1}{D} + 1\right) + G$, which will be the DFT length of the equalizer. Let us now define two vectors, $\hat{\mathbf{x}}_j = [\mathbf{0}_{1\times M'}, 1, \mathbf{0}_{1\times L-M'-1}]^{\mathbf{T}}$ and $\tilde{\mathbf{x}}_j = [\mathbf{0}_{1\times Z'}, 1, \mathbf{0}_{1\times Z'}, 1, \ldots]$, where $M' = \text{mod}\left(j - \lfloor \frac{j}{D} \rfloor - 1, N_T\right) K' + \lfloor \frac{j - \lfloor \frac{j}{D} \rfloor - 1}{N_T} \rfloor + \lfloor \frac{j}{D} \rfloor$ and $Z' = \frac{j - \frac{j}{D}}{N_T} + \frac{j}{D} - 1$. Then following the expression of Eq. (3), the transmitted layers over the N_T antennas with IAD can be written as

$$b' = \mathbf{W}_{\text{IAD}}\mathbf{s}, \tag{6}$$

where the transformation matrix for IAD can be written as

$$\mathbf{W}_{\text{IAD}} = [\hat{\mathbf{x}}_1, \hat{\mathbf{x}}_2, \ldots, \tilde{\mathbf{x}}_D, \hat{\mathbf{x}}_{D+1}, \ldots, \tilde{\mathbf{x}}_{2D}, \ldots, \tilde{\mathbf{x}}_{\gamma D}]\,, \tag{7}$$

where $\gamma = N_T Q/D$ is an integer. In this case, we assumed that the length of the coded symbol sequence $\mathbf{s}$, which is $N_T Q$, is divisible

[1] A generalized doping ratio can be define as $x : D$, where x can be any integer. However, $x > 1$ is not considered in this paper

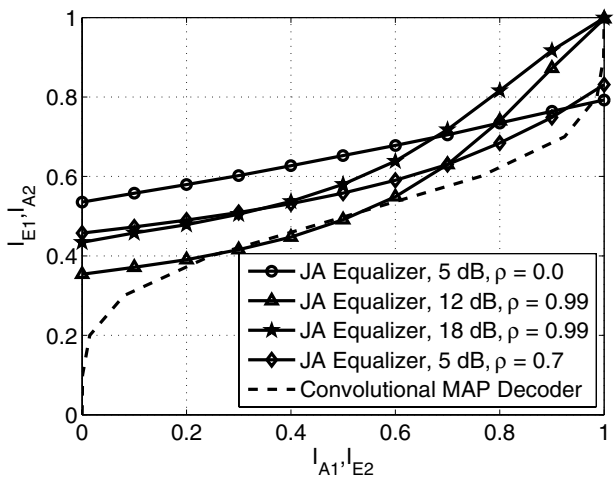

Fig. 4: EXIT chart of the JA turbo equalization with IAD doping ratio 1:5 at spatial correlation $\rho = 0.0, 0.99$ and 0.7.

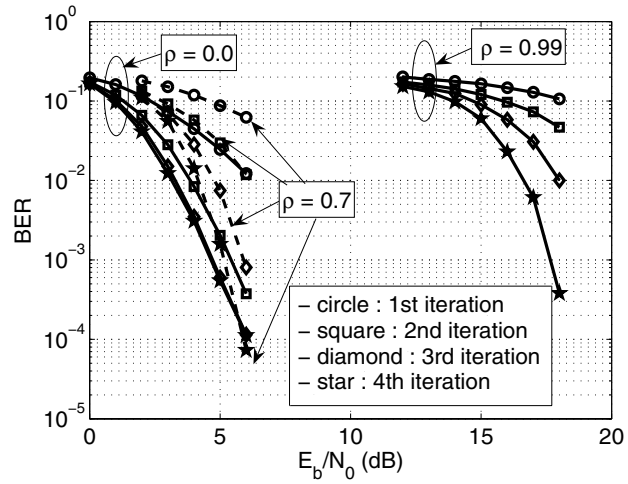

Fig. 5: BER performance of the SM system with IAD doping ratio 1:5 under various spatial correlations.

by D. Otherwise, zero padding can be added to the sequence so that γ becomes an integer.

Since Eq. (6) has the same form as Eq. (3), the same JA turbo equalizer proposed in [9]–[11] can also be applied in detecting the transmitted symbols in IAD systems. However, there are two differences to take note of. Firstly, instead of $N_T K$, the DFT length of the equalizer is now L. Secondly, for the doping symbols, the spatial MAP technique employed by the JA equalizer needs only to compute 2^M distance metrics for each possible bit candidate, where M is the number of bits per symbol. In contrast, $2^{N_T M}$ distance metrics have to be computed for the non-doping symbols, similar to the conventional SM case. In this paper, we have assumed that both the transmitter and the receiver know exactly the doping ratio that was adopted.

Let us now examine how the inclusion of IAD has alter the transfer characteristics of the JA equalizer. The same set of simulation parameters, given in Table I is used. The bandwidth expansion factor, as governed by Eq. (5), has been taken into account in our simulations. Fig. 4 shows the EXIT chart of the SM system with IAD for a doping ratio of 1:5; that is, one out of five symbols is a doping symbol. First of all, similar to the conventional SM system, a wide tunnel is observed at 5 dB when $\rho = 0.0$ with IAD, leading to similar convergence behavior. However, in the case of IAD, the BER performance will be limited, since the transfer characteristic of the JA equalizer intersects with that of the convolutional MAP decoder at $I_{E2} \approx 0.95$. Recall that the pinch-off limit without doping when $\rho = 0.99$ is around 18 dB. However, according to Fig. 4, a wide tunnel can now be seen at 18 dB when $\rho = 0.99$, which suggests that decoding convergence can be initiated. Thus, this clearly shows that IAD 'raises' up the transfer characteristic of the JA equalizer, thereby creating a tunnel and hence permitting further iterations. The pinch-off limit when $\rho = 0.99$ is now at about 12 dB. Also, at 5 dB when $\rho = 0.7$, the tunnel becomes wider with IAD as compared to the one without doping (see Fig. 2). Hence convergence with IAD is expected to be faster. Again, these claims can be substantiated by observing the BER performance, as shown in Fig. 5. Now, we can see that at 18 dB when $\rho = 0.99$, the BER is low because decoding convergence is possible. Furthermore, the pinch-off limit is in the region of 11-12 dB, which agrees with our observation from the EXIT chart. Comparing the BER with and without doping at

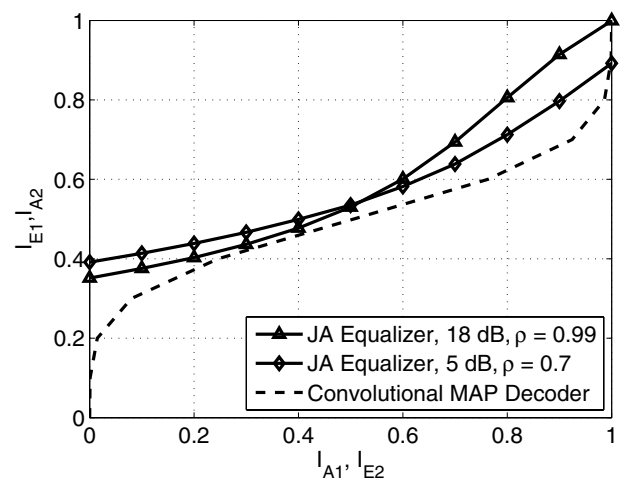

Fig. 6: EXIT chart of the JA turbo equalization with IAD doping ratio 1:33 at spatial correlation $\rho = 0.99$ and 0.7.

$\rho = 0.99$, we can see that the performance improved by about 3-4 dB at a BER of 10^{-3}. On the other hand, the BER of non-doping system at $\rho = 0.0$ is lower that that with IAD, which agrees with our previous observation of the EXIT chart. Also, at 5 dB when $\rho = 0.7$, the BER with IAD converges at a faster rate as compared to one without doping (see Fig. 3). This is due to a wider tunnel when IAD is invoked, which accelerated the convergence.

A doping ratio of 1:5 suffers a 37.5% loss in spectral efficiency, according to Eq. (5), while providing an improvement in the performance by triggering (creating a tunnel) or accelerating (widening the tunnel) convergence. Let us now consider a doping ratio of 1:33, which only results in a spectral efficiency loss of 8.3%. The EXIT chart and the BER performance is illustrated in Fig. 6 and Fig. 7, respectively. The BER performance with doping ratio 1:33 and without doping, as shown in Fig. 3 looks very similar, except for some very subtle differences upon close examination. For example, looking at the EXIT chart for $\rho = 0.99$ at 18 dB, we can see a very narrow tunnel is created with a doping ratio of 1:33, as compared to the one without doping as shown in Fig. 2. Because of this tunnel,

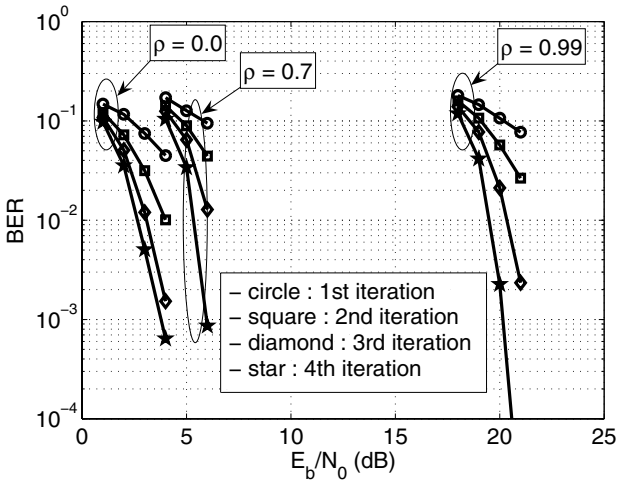

Fig. 7: BER performance of the SM system with IAD doping ratio 1:33 under various spatial correlations.

further iterations will lower the BER, albeit slowly, as can be seen in Fig. 7. Hence, if the number of iterations goes to infinity, optimal performance can be achieved. Similarly, comparing the EXIT charts of Fig. 2 and Fig. 6 when $\rho = 0.7$ at 5 dB, we can see that with a doping ratio of 1:33, the transfer characteristic of the JA equalizer raises up slightly when $I_{A1} = 0$ as compared to the one without doping. This slight rise enables the convergence to accelerate faster, resulting in a lower BER (compare Fig. 7 and Fig. 3).

In summary, the benefits of IAD is as follows: In the presence of high spatial correlation, the doping symbols, which are transmitted from all the antennas, are still co-phased and summed at the receiver side, resulting in a higher SNR gain. Hence the transfer characteristic of the JA equalizer will raise up, which will create, or widens a tunnel and initiates or accelerates convergence. The amount by which the transfer characteristic is raised is controlled by the doping ratio. The higher the doping ratio, the more the transfer characteristic raises. On the other hand, a higher doping ratio leads to a greater loss in the spectral efficiency. Hence IAD offers a nice tradeoff between convergence speed and information rate loss. Since the spatial correlation may vary with time, in order to optimize this tradeoff, adaptive doping ratio control can be implemented, whereby the receiver determines and feedback the appropriate doping ratio to be used to the transmitter, depending on the degree of spatial correlation. This implies that the receiver must know the degree of correlation, which can be estimated using methods proposed in [15].

B. Outer Perfect Antenna Doping

The structure of the SM transmitter with outer perfect AD (OPAD) is shown in Fig. 1(c). During the doping period ('ON' state), pilot symbols are passed to the encoder as well as transmitted from the antennas. Hence *a priori* information received directly from the channel are readily available to the decoder at the receiver end. This will have the effect of shifting the transfer characteristic of the decoder to the right (see Figs. 2, 4), where the amount of shift is determine by the doping ratio. Thus, OPAD has a different effect as compared to IAD, which raises up the transfer characteristic of the equalizer. By visualizing from the EXIT charts given in this paper, shifting the transfer characteristic of the decoder to the right can also create a tunnel that enables convergence to occur. Unfortunately, due to space limitation, OPAD will not be covered in detail in this paper.

V. Conclusions

A novel so-called antenna doping scheme has been proposed for MIMO SM transmission systems in the presence of transmit spatial correlation. In particular, IAD is thoroughly studied. With the aid of EXIT charts, we have shown that IAD alters the transfer characteristics of the JA equalizer such that a tunnel is created, which initiates decoding convergence. The results shown that the BER performance can be improved in correlated channels by incorporating IAD into the SM system.

References

[1] I. E. Telatar, "Capacity of multi-antenna gaussian channels," *Eur. Trans. Telecommun.*, vol. 10, no. 6, pp. 585–595, Nov. 1999.

[2] G. J. Foschini, and M. J. Gans, "On limits of wireless communications in a fading environment when using multiple antennas," *Wireless Pers. Commun.*, vol. 6, pp. 311–335, Mar. 1998.

[3] D. Shiu, G. J. Foschini, M. J. Gans, and J. M. Kahn, "Fading correlation and its effect on the capacity of multi-element antenna systems," *IEEE Trans. Commun.*, vol. 48, no. 3, pp. 502–513, Mar. 2000.

[4] D. A. Gore, R. W. Heath Jr., and A. J. Paulraj, "Transmit selection in spatial multiplexing systems," *IEEE Commun. Lett.*, vol. 6, no. 11, pp. 491–493, Nov. 2002.

[5] R. Narasimhan, "Spatial multiplexing with transmit antenna and constellation selection for correlated MIMO fading channels," *IEEE Trans. Signal Processing*, vol. 51, no. 11, pp. 2829–2838, Nov. 2003.

[6] A. F. Molisch, and X. Zhang, "FFT-based hybrid antenna selection schemes for spatially correlated MIMO channels," *IEEE Commun. Lett.*, vol. 8, no. 1, pp. 36–38, Jan. 2004.

[7] R. U. Nabar, H. Bölcskei, and A. J. Paulraj, "Transmit optimization for spatial multiplexing in the presence of spatial fading correlation," in *Proc. IEEE Globecom*, San Antonio, TX, pp. 131–135, Nov. 2001.

[8] J. Akhtar, and D. Gesbert, "Spatial multiplexing over correlated MIMO channels with a closed-form precoder," *IEEE Trans. Wireless Commun.*, vol. 4, no. 5, pp. 2400-2409, Sept. 2005.

[9] J. Karjalainen, K. Kansanen, N. Veselinovic, and T. Matsumoto, "Antenna-by-antenna and joint-over-antenna MIMO signal detection techniques for turbo-coded SC/MMSE frequency domain equalization," in *Proc. IEEE Spring Veh. Technol. Conf. (VTC)*, Stockholm, Sweden, pp. 934–938, May 2005.

[10] J. Karjalainen, K. Kansanen, N. Veselinovic, and T. Matsumoto, "Frequency domain joint-over-antenna MIMO turbo equalization," in *Proc. Annual Asilomar Conf. Signals, Syst., Comp.*, Pacific Grove, USA, Oct. 2005.

[11] J. Karjalainen, K. Kansanen, N. Veselinovic, and T. Matsumoto, "Iterative frequency domain joint-over-antenna receiver for multiuser MIMO," in *Proc. Int. Symb. on Turbo Codes*, Munich, Germany, Apr. 3–7 2006.

[12] S. ten Brink, "Code doping for triggering iterative decoding convergence," *Proc. IEEE Int. Symp. Inform. Theory*, pp. 235, Jul. 2001.

[13] S. ten Brink, "Designing iterative decoding schemes with the extrinsic information transfer chart," *AEÜ Int. J. Electron. Commun.*, vol. 54, no. 6, pp. 389–398, Dec. 2000.

[14] D. Falconer, S. Ariyavisitakul, A. Benyamin-Seeyar, and B. Eidson, "Frequency domain equalization for single-carrier broadband wireless systems," *IEEE Commun. Mag.*, vol. 40, no. 4, pp. 58–66, Apr. 2002.

[15] J. H. Kotecha, and A. M. Sayeed, "Transmit signal design for optimal estimation of correlated MIMO channels," *IEEE Trans. Signal Process.*, vol. 52, no. 2, pp. 546–557, Feb. 2004.